



---

## Eight-switch Converter using PMSG Based WECS for Stand-alone Applications

---

Fatma Selim, Mohamed Z. Youssef and Mohammed Orabi

EasyChair preprints are intended for rapid dissemination of research results and are integrated with the rest of EasyChair.

December 14, 2019



# Eight-switch Converter using PMSG Based WECS for Stand-alone Applications

Fatma Selim\*, Mohamed Z. Youssef\*\*, Mohammed Orabi\*

\*APEARC, Aswan University, Aswan 81542, Egypt

\*\* University of Ontario Institute of Technology, Oshawa ON L1G 0C5, Canada

[morabi@apearc.aswu.edu.eg](mailto:morabi@apearc.aswu.edu.eg)

**Abstract**— this paper introduces a study of stand-alone variable speed small wind energy conversion system (WECS) using eight-switch converter to fulfill a satisfied minimizing of power switches reaches to 20 % less than the B-2-B converter by using new PWM technique to generate the gating pulses for power switches. In addition, the PWM technique has proved the ability to simplify the control strategy. Maximum power is extracted by controlling the three-phase boost converter. Inverter is controlled to maintain the load voltage and the load frequency to be constant. Battery energy storage system (BESS) is used to fix the dc-bus voltage and compensating the load power by using a reliable control technique based on the pulse width modulation (PWM). To validate the proposed topology, the simulation results show that the proposed topology outperforms the state-of-the-previous topologies in terms of reducing power elements and simplifying the control structure.

**Keywords**— Small wind energy conversion system (SWECS), Permanent magnet synchronous generator (PMSG), Battery energy storage system (BESS), Maximum power point (MPP).

## I. INTRODUCTION

Due to the increasing concern about the conventional generation units, such as the depletion of fossil fuels, and the negative impact on the environment like the air pollution, this encourages the researchers' trends to the exploitation of renewable energy sources.

Renewable energy sources, such as wind turbine (WT), solar cell and Photovoltaic (PV) systems are naturally replenished on a human timescale due to their numerous advantages such as sustainability and low environmental impacts. by virtue of renewable energy, the poorest nations have been lifted to new levels of prosperity. Photovoltaic and wind generation schemes are considered the most economic choices because they lead to a significant reduction in primary energy requirements, because most renewables don't have a steam cycle with high losses.

The fast progress in power electronics technologies helping in combining renewable energy sources and distributed generators into the utility grid, as well as presenting new strategies for the operation and management of the electricity grid, in addition to improving the power-supply reliability, quality and liberalization of the grids, all those factors lead to new management structures. The matter with small wind turbine rather than regular wind system is the cost which is relevant to the number of the power switches. Therefore, it is targeted to develop an improved topology for wind energy with

less power electronics element count and thus less gate driver circuits and less circuit layout complexity.

Although the back-to-back converter has proved the reliability and has shown an outstanding performance of WECS, it still requires many power switches that reached to 12-switch like MOSFETs or IGBTs. As well as a large value of DC-link capacitor for filtering the Dc voltage have been needed, several attempts have been previously proposed so as to get rid of these obstacles [1]. Hence, a less-number of components with reduced cost have been needed to achieve high efficiency should be realized. In this paper, we propose a new topology to perform the previous requirements. Simulation results are introduced so as to prove the reliability of the proposed topology and its ability to control the load voltage prominently showing the advantages of the integration of the BESS to the wind system [2-5].

## II. SYSTEM CONSTRUCTION

Fig. 1 shows the structure of proposed eight-switch converter topology. This converter has three legs, the first two legs consists of three power switches and the third leg has only two power switches. The proposed topology has achieved 20 % cost saving as it saves about also 20 % of power switches. The three middle switches are shared with the lower ones to operate as a rectifier and only the two middle switches of the first two legs are shared with the upper ones to act as an H-bridge inverter, hence the input power transferred through the three bottom switches and the three middle switches to the DC-link (rectification stage) and then from the DC-link to the stand-alone load through the H-bridge DC/AC converter (inversion stage) [6-10]. So, the challenge here is to maintain a control strategy which to have the ability to obtain the maximum power from the wind to cover the load demand. There are two modes of operations for the proposed converter:

The first mode: is called a constant frequency mode (CF), in this mode the load frequency is kept constant and is equal the line or fundamental frequency, but the load inverter voltage can vary with the variation of the inverter modulation index.

The second mode is a variable frequency mode (VF), in this mode both load frequency with the load voltage are being variable. Here we apply the constant frequency mode as the sine wave output frequency is constant.

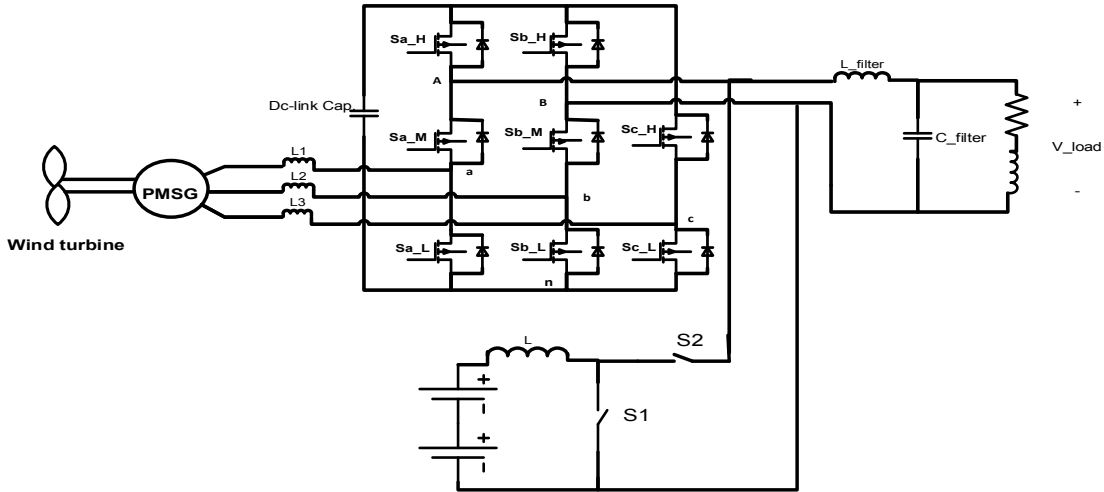


Fig. 1. Proposed eight-switch converter topology.

### III. CONVERTER MODULATION SCHEME

The control scheme of the eight-switch topology can be achieved through controlling the all switches in the three legs, and to insure the reliability of the proposed control strategy it must that the three switches in the same leg couldn't operate in the same time the matter that makes the proposed converter having three switching states unlike the back to back converter that it shown in fig. 2 which has four switching states as they are listed in table I, according to the switching states of eight-switch converter which are listed in table II at any case the rectifier modulation signal shouldn't be higher than the inverter modulation signal at any instant. Fig.3 explains the modulation scheme of the proposed converter, the modulation signal of the inverter and the rectifier are compared with a single carrier by adding a proper offset for both signals so as to prevent the interference that may occur between them, hence the inverter modulation signal shouldn't be lower than the rectifier one [11].

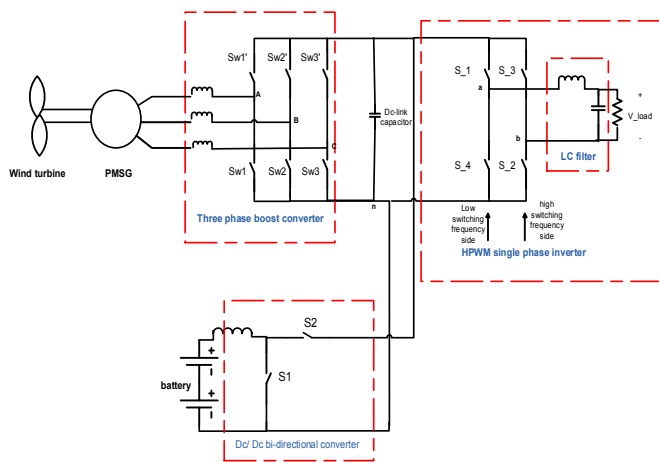


Fig. 2. back to back converter topology [7].

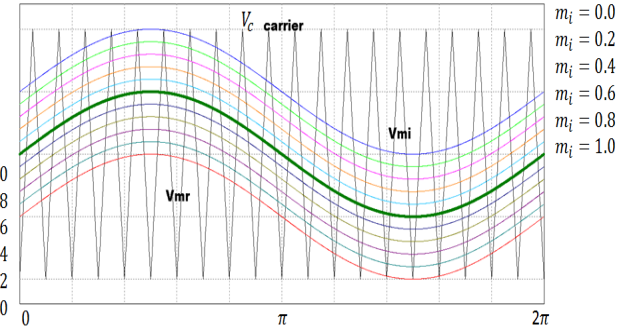


Fig. 3. modulation scheme through single switching period for the eight-switch converter[10].

TABLE I. SWITCHING STATE FOR BACK TO BACK CONVERTER.

Back to back converter						
Switching stat	Sw1'	Sw1	S_1	S_4	V <sub>An</sub>	V <sub>an</sub>
1	On	Off	on	off	V <sub>dc</sub>	V <sub>dc</sub>
2	off	On	off	on	0	0
3	On	Off	off	on	V <sub>dc</sub>	0
4	off	On	on	off	0	V <sub>dc</sub>

TABLE II. SWITCHING STATES FOR PROPOSED 8-SWITCH CONVERTER.

Proposed 8-switch converter					
Switching state	Sa_H	Sa_M	Sa_L	V <sub>An</sub>	V <sub>an</sub>
1	On	on	off	V <sub>dc</sub>	V <sub>dc</sub>
2	Off	on	off	0	0
3	On	off	off	V <sub>dc</sub>	0

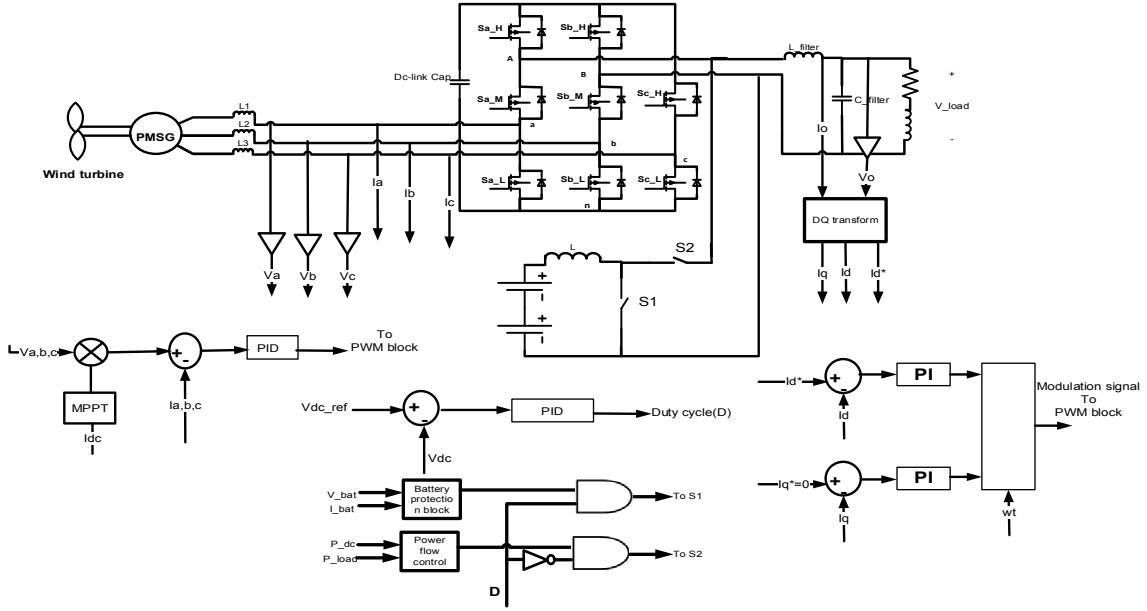


Fig. 4. schematic diagram of control system.

#### IV. CONTROL STRATEGY FOR THE SYSTEM

Fig. 4 includes schematic diagrams for the control process that happens in each part of the system. First maximum power is extracted from the wind by sensing the DC current only as the DC voltage is maintained constant from the bi- directional converter regulation so, this current is connected to a MPPT block to generate the maximum current then this current is multiplied by the shapes of the generator phase voltages to obtain the reference currents which is compared with the measured current in order to achieve the unity power factor. After that the modulation signals are generated from PID controller to be subjected to the PWM block. Second is controlling the load voltage with the frequency and it is achieved by using the d-q transformation.

Third is regulating of the DC-link voltage by controlling the bi-directional converter, this control is divided into three functions first of them is to make a power flow control (power management) as if the power comes from the wind is higher than the load demand (at light loads) the extra power is charged into the battery through the converter, also if the wind power is smaller than the load power the battery discharges through the Dc-link to cover the demand (at high demands). The second function is to prevent the battery from a deep discharging or the overcharging through the battery protection block, and finally regulating the Dc voltage. So, the battery has two mode for discharging and two modes for discharging. Fig. 5 explains the modes of operation of the bi-directional converter, as described below mode\_1 indicates the case that the battery is discharging through the inductor through Q2, moving on mode\_2 we find that the battery is discharging through the anti-parallel diode of switch Q1 to the dc bus in case of the two switches are in the off state. Moreover, mode\_3 explains the charging process of

the battery through switch Q1 and mode\_4 the charging of the battery from the conductor energy through the anti-parallel diode of switch Q2. For a conclusion the process of discharging occurs during mode\_1 & mode\_2 and the charging process occurs during mode\_3 & mode\_4 the manner which has been clarified in the Table III [12].

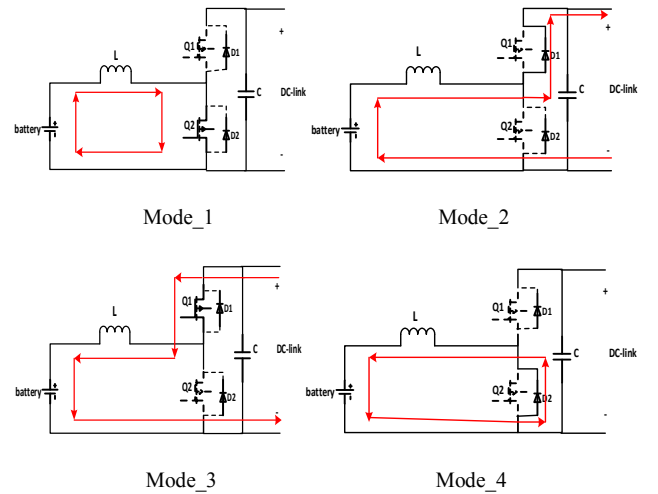


Fig. 5. Modes of operation of the bi-directional converter [12].

TABLE III. CHARGING AND DISCHARGING PROCESS OF THE BATTERY THROUGH THE BI-DIRECTIONAL CONVERTER.

Mode	Switching states				Process of the battery
	Q1	D1	Q2	D2	
Mode 1	off	off	on	Off	Discharging
Mode 2	off	on	off	Off	Discharging
Mode 3	on	off	off	Off	Charging
Mode 4	off	off	off	On	Charging

Fig. 6 illustrates what happens in the PWM block which explains the sinusoidal pulse width modulation scheme of the proposed converter and the resultant switching states. Here, there is one reference signal for each leg in the rectifier side ( $V_{mr}$ ) and two for the inverter side ( $V_{mi}$ ). The rectifier reference signals mustn't exceed the reference signals of the inverter ( $V_{mi} > V_{mr}$ ). This is fulfilled by inserting adequate offsets to both references signals, so as to get rid of the signals overlapping. So, it results in that to raise the modulation of the inverter you should keep the modulation of the rectifier low.

Consequently, three modulation signals are obtained for two legs and two modulation signals are obtained for the third leg. These modulation signals will be compared to a single high frequency carrier which has been shown in Fig. 6 to obtain the switches gating signals as it has been described in the diagram which shown in Fig. 7. The gating signals of the first two middle switches (first two legs) are resulted from the logical NANDs of the gating signals of the upper switches with ones in the lower each in the same leg as shown in Fig. 7 [6]. The third switch gating signal comes from the logical NOT of the lower switch gating signal in the same leg. Hence, the availability of a shoot-through state is prevented.

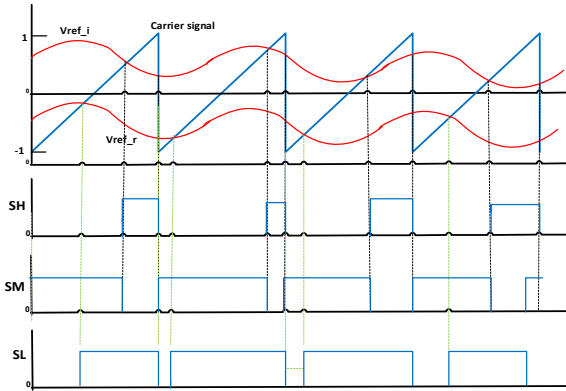


Fig. 6. PWM method for the proposed 8-switch Ac/ac converter[6].

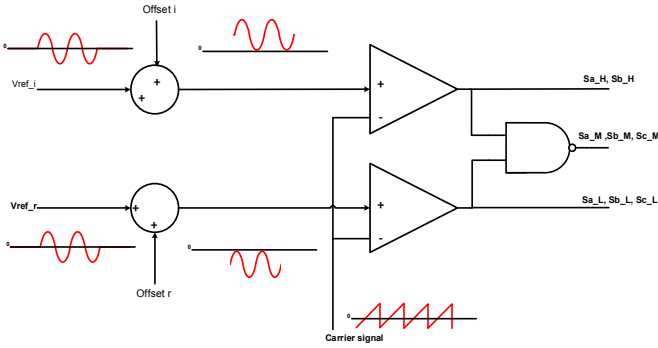


Fig. 7. Block diagram of generation of the gating signals.

As it has been declared above that the proposed converter has two modes of operation and they are constant frequency mode & variable frequency mode and Here we apply the constant frequency mode as the sine wave output frequency is constant. Table IV Summarize the two modes below.

TABLE IV. TWO MODES OF PWM OPERATION FOR PROPOSED 8-SWITCH CONVERTER.

	First Mode (CF)	Second Mode (VF)
Upper and lower offset limits	$\text{offset}_i = 1-m_i$ $\text{offset}_r = m_r-1$	$\text{offset}_i + \text{offset}_r \leq 1$ $\text{offset}_i = 1-\alpha$ $\text{offset}_r = -\alpha$ where: $\alpha = \frac{m_i}{m_r+m_i}$
Maximum modulation index	$m_i \leq 1$ $m_r \leq 1$	$m_i+m_r \leq 1$ $m_i \leq 1$ $m_r \leq 1$

## V. RESULTS AND DISCUSSION

So as to insure the reliability and the capability of the system with eight power switches for the AC/AC converter to fulfill all the demand requirements which are extracting maximum power from the wind input and fulfilling unity power factor as well as covering the load demand and also compensating the load power, The whole system has been built on PSIM software as described in Fig. 4 which shows the circuit under study with reduced number of power switches. The whole values of the system parameters have been inserted into table V, and it is obviously cleared that the capacitor value of the DC-link has been decreased to be a quarter less than that used in the previous topology in [8]. The system performance under step change of wind speed has been presented into the results so as to insure the adequacy of the control system under the variation of the input wind power.

TABLE V. DESIGN PARAMETERS FOR SYSTEM SIMULATION.

Parameters	Values
Wind turbine power rating	1.0 kW
Rated wind speed	10 m/s
Load RMS Voltage	220Vac
Battery voltage	120 V
dc-link voltage	400 Vdc
Output ac load voltage frequency	50Hz
Bi-directional converter switching frequency	25kHz
Inverter switching frequency	10kHz
Input three phase LC filter	1.0mH and 100 $\mu$ F
<b>dc-link capacitor value</b>	<b>0.5 mF</b>
Bi-directional converter inductance	1.68mH
Load LC filter	1.0mH and 4 $\mu$ F

The simulation results have approved the reliability and the efficiency of the proposed topology for converting the variable wind power to a constant AC load power with a less number of power switches that leads to low system cost with less weight and high efficiency.

Fig. 8 indicates the step variation occurs in wind speed from low speed to speed over the rated one until reaching to the rated speed, according to this variation the input power being changed and this has been appeared across the speed RPM of the generator that changes with the same scenario of the wind speed in Fig. 9.

Fig. 10 shows the PWM carrier with the modulation signals of the inverter ( $d_1$ ), the other modulation signal of the inverter comes from shifting the first signal ( $d_1$ ) by a phase shift of  $180^\circ$  degree and the three modulation signals of the converter ( $m_1, m_2, m_3$ ). Fig. 11 shows a zooming in for Fig. 10.

In addition to the variation of the three phase voltages with their phase currents that have been cleared through fig. 12 and fig. 13, the matter which indicates the tracking efficiency and the reliability of the MPP control for obtaining the maximum power of the wind at any case of wind speed changes. The zooming in has been done on these figures through fig. 14 and fig. 15

Fig. 16 summarizes the voltage stress that occurs on the three switches in each leg of the converter. So, it could be noticed that the value of the maximum stress voltage is equal to the dc-link voltage. The matter which clarifies the reliability of the proposed topology than the back to back converter as the same switches rating can be used in this topology, the matter which effect on the reduction of the total power switches cost.

Fig. 17 indicates the dc modulation signal of the bi-directional converter. And Fig. 18 clarifies the bi-directional switches duty cycles it can be noticed that the two switches operate in contrary. Moving to Fig. 19 that indicates the wave shape of the dc-link voltage which remains at a constant value so as to not to affect the load voltage regulation that the wave shape of it is clarified in Fig. 20 with its load current. The FFT analysis of inverter output voltage before the filter and load voltage after filtering are shown in Fig. 21 respectively. It is clear that the magnitude of harmonic at switching frequency (10 kHz) for the inverter unfiltered voltage is about 24 % and for the load filtered voltage is about 2.2%.

Fig. 22 indicates the battery current cases from discharging and charging to and from the dc- link according to the input power variation from being under the load power demand to being over the load power demand. And this could be obviously clarified through Fig. 23 that shows the wave shapes of the two input powers (wind power +battery power) and the load power of the inverter that clarify the compensation process that occurs on the load power.

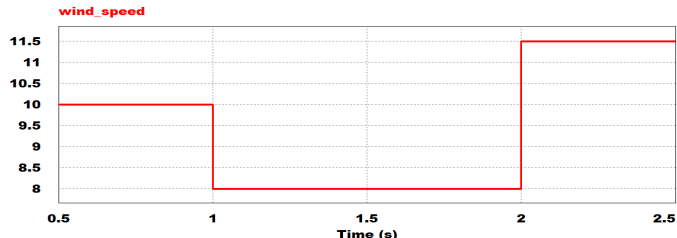


Fig. 8. Step change of the wind speed from 10 m/s to 8 m/s and 11.5 m/s.

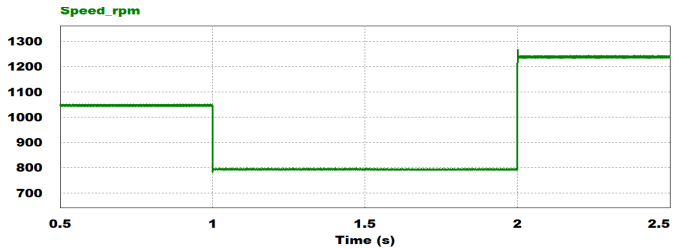


Fig. 9. Speed RPM of generator during the change of the input speed.

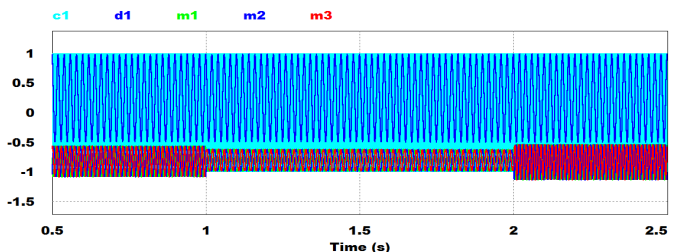


Fig. 10. Carrier signal ( $c_1$ ) is compared with modulation signal of inverter ( $d_1$ ) and the three phase modulation signals of converter ( $m_1, m_2, m_3$ ).

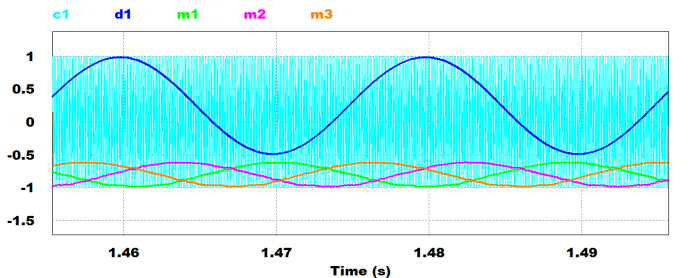


Fig. 11. Zooming in of the carrier signal ( $c_1$ ) is compared with the modulation signal of the inverter ( $d_1$ ) and the three phase modulation signals of the converter( $m_1, m_2, m_3$ ).

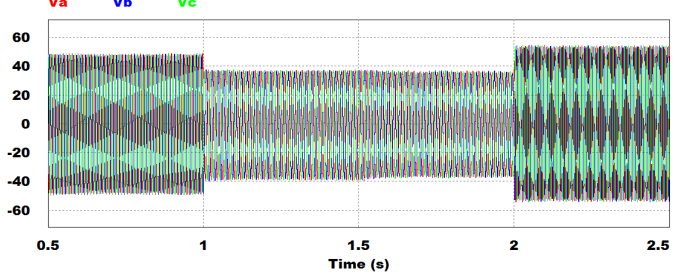


Fig. 12. The three phase generator voltages according to the variation of the input power.

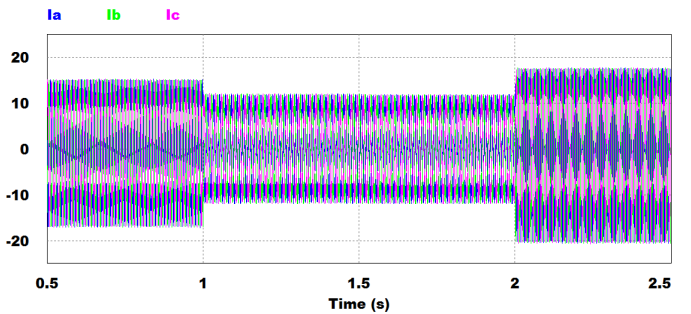


Fig. 13. The three phase generator currents according to the variation of the input power.

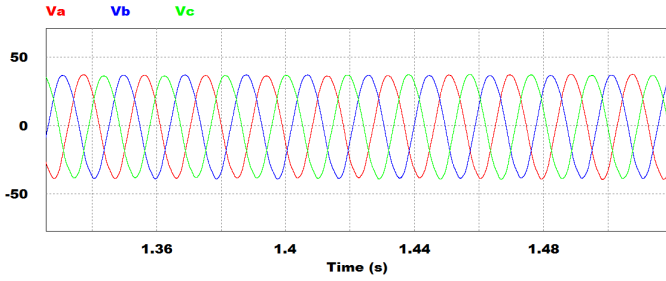


Fig. 14. Zooming in of the three phase generator voltages according to the variation of the input power.

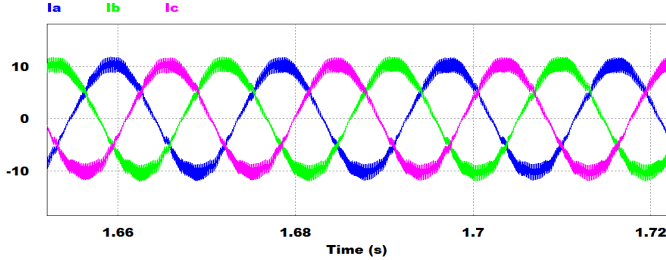
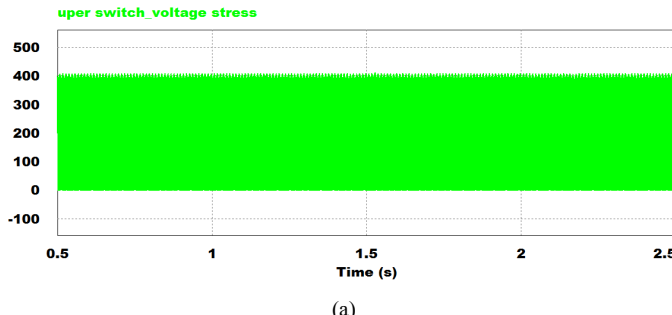
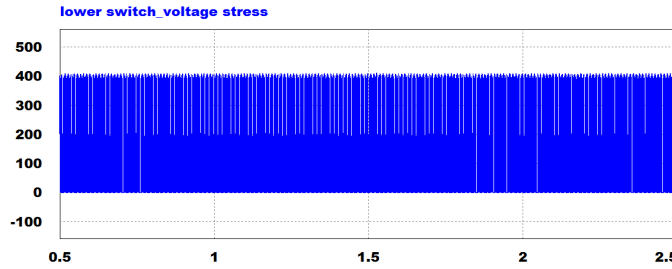


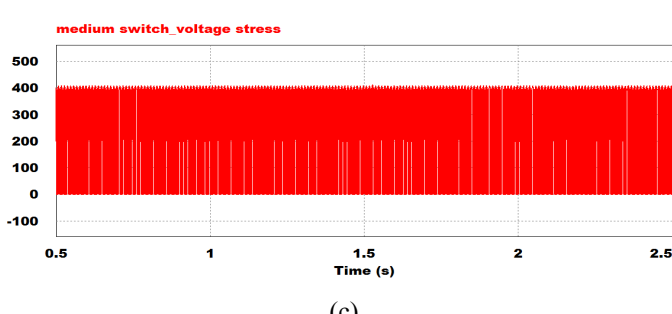
Fig. 15. Zooming in of the three phase generator currents according to the variation of the input power.



(a)



(b)



(c)

Fig. 16. The voltage stress of the switches of the AC/AC 8-switches converter (a) Upper switches (b) Lower switches (c) Medium switches.

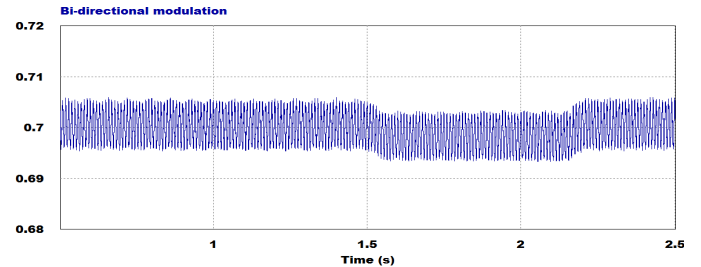


Fig. 17. The modulation signal of the DC/DC bi-directional converter.

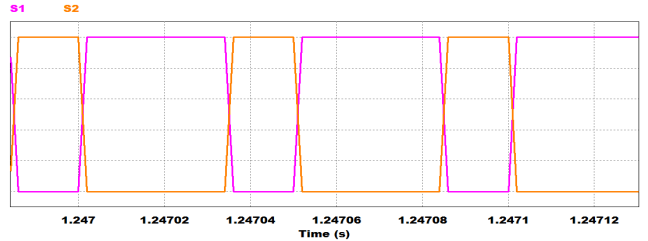


Fig. 18. The duty cycle of the bi-directional converter.

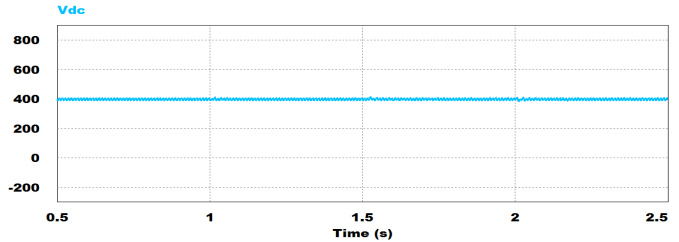


Fig. 19. The DC-link voltage through the change in wind speed.

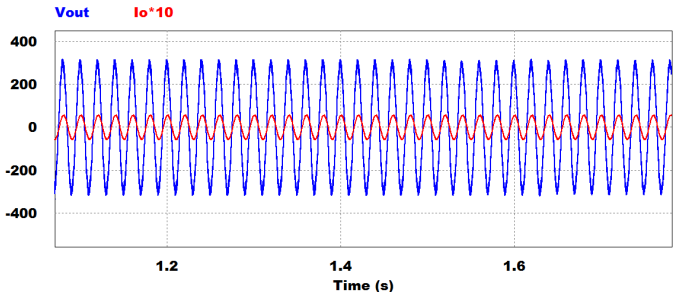


Fig. 20. Load voltage with its load current in case of input power variation.

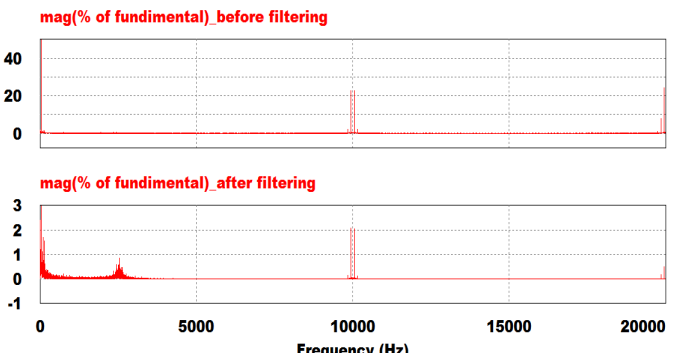


Fig. 21. FFT analysis of the output unfiltered and the filtered inverter voltage in the eight switch topology.

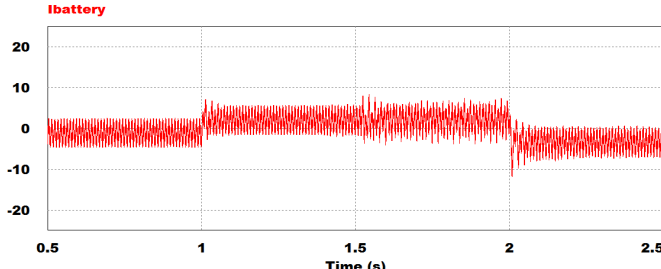


Fig. 22. Battery current waveform in case of discharging, charging to the DC-bus and in case of balancing..

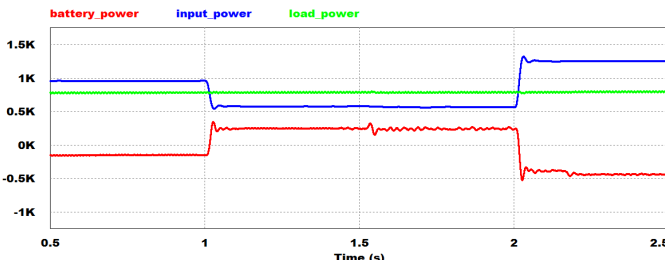


Fig. 23. The input powers (wind power +battery power) and the load power of the inverter.

## VI. CONCLUSION

The proposed paper has introduced a new reduced switch count of AC/AC converter reconstruction based on eight switches power converter. The topology can be considered as a successful one from reducing the cost and the weight of the WECS. This topology is used for maximum power tracking control and delivering power to the load, simultaneously. The proposed system is simple and has cost advantages compared to conventional WECS, because the number of switching semiconductors is reduced to eight and also, the maximum voltage stress of the power switches remains as the same value in the back to back converter. The THD analysis for the output inverter voltage has been cleared through the results. Also, the effectiveness of the operation of the proposed converter and its ability to track the maximum power operating point of WES without rotor speed sensor in transient conditions were demonstrated by simulation results.

## REFERENCES

- [1] Y. Du and A. K. S. Bhat, "Power Converter Schemes for Small Scale Wind Energy Conversion Systems - Review, a Systematic Classification Based on Isolation Transformer and Generator Side Rectifier," in 2016 Second International Conference on Computational Intelligence & Communication Technology (CICT), 2016, pp. 338-344.
- [2] A.-R. Haitham, M. Mariusz, and A.-H. Kamal, "Energy, Global Warming and Impact of Power Electronics in the Present Century," in Power Electronics for Renewable Energy Systems, Transportation and Industrial Applications, ed: IEEE, 2014, p. 1.
- [3] J. Joo, S. Raghavan, and Z. Sun, "Integration of Sustainable Manufacturing Systems into Smart Grids with High Penetration of Renewable Energy Resources," in 2016 IEEE Green Technologies Conference (GreenTech), 2016, pp. 12-17.
- [4] X. Liang, "Emerging Power Quality Challenges Due to Integration of Renewable Energy Sources," IEEE Transactions on Industry Applications, vol. 53, pp. 855-866, 2017.
- [5] B. Kroposki, C. Pink, R. DeBlasio, H. Thomas, M. Simões, and P. K. Sen, "Benefits of Power Electronic Interfaces for Distributed Energy Systems," IEEE Transactions on Energy Conversion, vol. 25, pp. 901-908, 2010.
- [6] M. Heydari, A. Y. Varjani, M. Mohamadian, and H. Zahedi, "A novel variable-speed wind energy system using permanent-magnet synchronous generator and nine-switch AC/AC converter," in 2011 2nd Power Electronics, Drive Systems and Technologies Conference, 2011, pp. 5-9.
- [7] T. Kominami and Y. Fujimoto, "A Novel Nine-Switch Inverter for Independent Control of Two Three-Phase Loads," in 2007 IEEE Industry Applications Annual Meeting, 2007, pp. 2346-2350. Vikrant.A.Chaudhari, July 2005. Automatic peak power tracker for solar PV modules using dSPACER software. Maulana Azad national institute of technology, Deemed University. BHOPAL – 462007.
- [8] F. Selim, E. M. Ahmed, M. A. Sayed and M. Orabi, "Stand-alone Small Wind Energy Conversion System with Reduced Sensors Control," Intelec 2013; 35th International Telecommunications Energy Conference, SMART POWER AND EFFICIENCY, Hamburg, Germany, 2013, pp. 1-6.
- [9] A. Fatemi, M. Azizi, M. Shahparasti, M. Mohamadian, and A. Yazdian, "A Novel Single-phase six-switch AC/AC converter for UPS applications," in Power Electronics, Drive Systems and Technologies Conference (PEDSTC), 2011 2nd, 2011, pp. 408-414.
- [10] F. Gao, L. Zhang, D. Li, P. C. Loh, and Y. Tang, "Optimal pulselwidth modulation of nine-switch inverter," in Power Electronics and Drive Systems, 2009. PEDS 2009. International Conference on, 2009, pp. 718-723.
- [11] M. K. Sahu and S. Bharti, "Simulation of three phase three leg Ac/Ac converter using Svpwm with six pulses," in Intelligent Systems and Control (ISCO), 2014 IEEE 8th International Conference on, 2014, pp. 155-160.
- [12] M. M. Hussein, T. Senju, M. Orabi, M. A. Wahab, and M. M. Hamada, "Control of a stand-alone variable speed wind energy supply system," Applied Sciences, vol. 3, pp. 437-456, 2013.